

Supporting Information

Benzoate Acid-Dependent Lattice Dimension of Co-MOFs and MOF-Derived CoS₂@CNTs with Tunable Pore Diameters for Supercapacitors

Kang-Yu Zou, Yi-Chen Liu, Yi-Fan Jiang, Cheng-Yan Yu, Man-Li Yue and Zuo-Xi Li^{*}

Key Laboratory of Synthetic and Natural Functional Molecule Chemistry (Ministry of Education), Shaanxi Key Laboratory of Physico-Inorganic Chemistry, College of Chemistry and Material Sciences, Northwest University, Xi'an 710069, P.R.China

*Corresponding author. E-mail: Lizx@nwu.edu.cn

Supporting Information Index:

Table **S1** Selected Bond Lengths [Å] and Angles [°] for Co-MOFs **1-3**.

Table **S2** The accurate Co contents of all MOF-derived materials.

Table **S3** Specific capacitances of **CoS₂@CNTs**.

Fig. **S1** The adamantane cage with large edges in **3**.

Fig. **S2** The simulated and experimental XRD patterns of Co-MOFs **(a) 1; (b) 2; (c) 3**.

Fig. **S3** The Co 2p spectra and S 2p spectra of **(a, b)** (*o*)-**CoS₂@CNT**; **(c, d)** (*m*)-**CoS₂@CNT**.

Fig. **S4** The FESEM images of Co-MOFs **(a) 1; (b) 2; (c) 3**.

Fig. **S5** FESEM images of **(a, b)** (*o*)-**Co@CNT**; **(c, d)** (*m*)-**Co@CNT**; **(e, f)** (*p*)-**Co@CNT**.

Fig. **S6** EDX results of (*o*)-**CoS₂@CNT**.

Fig. **S7** EDX results of (*m*)-**CoS₂@CNT**.

Fig. **S8** EDX results of (*p*)-**CoS₂@CNT**.

Fig. **S9** TEM and HRTEM images of **(a, b)** (*m*)-**Co@CNT**; **(c, d)** (*p*)-**Co@CNT**.

Fig. **S10** TEM images of long high-quality CNTs in (*p*)-**Co@CNT**.

Fig. **S11** CV and GCD curves of **(a, b)** (*o*)-**CoS₂@CNT**; **(c, d)** (*m*)-**CoS₂@CNT**.

Fig. **S12** The Nyquist plots of Co-MOFs.

Fig. **S13** The Nyquist plots of **(a)** **Co@CNTs**; **(b)** **CoS₂@CNTs**.

Table S1 Selected Bond Lengths [Å] and Angles [°] for Co-MOFs **1-3**.

1			
Co(1)-O(2)	2.080(2)	Co(1)-O(4)#1	2.037(2)
Co(1)-O(1)	2.287(2)		
Co(1)-N(1)	2.071(2)	Co(1)-N(3)	2.080(2)
O(4)#1-Co(1)-O(2)	108.51(8)	N(1)-Co(1)-O(2)	104.20(9)
N(3)-Co(1)-O(2)	131.92(9)	O(4)#1-Co(1)-N(1)	91.61(9)
O(4)#1-Co(1)-N(3)	109.10(10)	N(1)-Co(1)-N(3)	103.58(10)
O(4)#1-Co(1)-O(1)	166.98(8)	N(1)-Co(1)-O(1)	84.91(9)
N(3)-Co(1)-O(1)	83.91(9)	O(2)-Co(1)-O(1)	60.55(7)
2			
Co(1)-O(7)#1	2.039(5)	Co(1)-O(2)	2.043(6)
Co(1)-O(1)	2.408(8)	Co(1)-O(8)	2.436(7)
Co(1)-N(1)	2.077(7)	Co(1)-N(4)#2	2.086(7)
Co(2)-O(3)	2.070(5)	Co(2)-O(5)	2.075(6)
Co(2)-O(4)	2.296(7)	Co(2)-O(6)	2.337(7)
Co(2)-N(8)#2	2.094(7)	Co(2)-N(5)	2.095(7)
O(7)#1-Co(1)-O(2)	150.0(3)	O(7)#1-Co(1)-N(1)	100.9(3)
O(2)-Co(1)-N(1)	99.7(3)	O(7)#1-Co(1)-N(4)#2	98.3(3)
O(2)-Co(1)-N(4)#2	98.2(3)	N(1)-Co(1)-N(4)#2	102.6(3)
O(7)#1-Co(1)-O(1)	97.9(3)	O(2)-Co(1)-O(1)	59.9(3)
N(1)-Co(1)-O(1)	159.6(2)	N(4)#2-Co(1)-O(1)	82.3(3)
O(3)-Co(2)-O(5)	159.8(3)	O(3)-Co(2)-N(8)#2	95.7(2)
O(5)-Co(2)-N(8)#2	98.0(2)	O(3)-Co(2)-N(5)	95.1(2)
O(5)-Co(2)-N(5)	96.3(3)	N(8)#2-Co(2)-N(5)	102.8(2)
O(3)-Co(2)-O(4)	59.4(2)	O(5)-Co(2)-O(4)	106.2(2)

N(8)#2-Co(2)-O(4)	88.2(2)	N(5)-Co(2)-O(4)	153.5(2)
O(3)-Co(2)-O(6)	104.1(2)	O(5)-Co(2)-O(6)	59.9(2)
N(8)#2-Co(2)-O(6)	156.8(2)	N(5)-Co(2)-O(6)	87.4(2)
O(4)-Co(2)-O(6)	91.7(2)		
	3		
Co(1)-O(3)	2.061(2)	Co(1)-O(1W)	2.148(2)
Co(1)-O(1)	2.199(2)	Co(1)-O(2)	2.225(2)
Co(1)-N(1)	2.127(2)	Co(1)-N(3)	2.099(2)
O(1)-Co(1)-O(2)	59.89(7)	O(3)-Co(1)-O(1)	168.23(7)
O(1W)-Co(1)-O(1)	84.47(7)	N(1)-Co(1)-O(1)	92.96(7)
N(3)-Co(1)-O(1)	96.57(8)	O(3)-Co(1)-O(2)	109.17(7)
O(1W)-Co(1)-O(2)	85.33(7)	N(1)-Co(1)-O(2)	86.83(8)
N(3)-Co(1)-O(2)	156.42(7)	O(3)-Co(1)-O(1W)	90.48(7)
O(3)-Co(1)-N(1)	90.60(7)	O(3)-Co(1)-N(3)	94.41(8)
N(1)-Co(1)-O(1W)	172.00(7)	N(3)-Co(1)-O(1W)	94.31(8)
N(3)-Co(1)-N(1)	93.51(8)		

Symmetry mode for **1**: #1 -x+1, y+1/2, -z+1/2. For **2**: #1 x, y+1, z+1; #2 x+1, y+1, z.

Table S2 The accurate Co contents of all MOF-derived materials.

Samples	Co (wt %)
(<i>o</i>)-Co@CNT	7.3
(<i>m</i>)-Co@CNT	8.9
(<i>p</i>)-Co@CNT	10.1
(<i>o</i>)-CoS ₂ @CNT	10.6
(<i>m</i>)-CoS ₂ @CNT	11.5
(<i>p</i>)-CoS ₂ @CNT	12.3

Table S3 Specific capacitances of CoS₂@CNTs at different scan rates and current densities.

Sample	Specific capacitance (F g ⁻¹)									
	Scan rate (mV s ⁻¹)					Current density (A g ⁻¹)				
	5	10	20	50	100	0.5	1	2	5	10
(<i>o</i>)-CoS ₂ @CNT	155	143	130	98	73	146	139	125	112	72
(<i>m</i>)-CoS ₂ @CNT	422	396	266	174	122	405	385	278	200	158
(<i>p</i>)-CoS ₂ @CNT	839	792	663	530	447	825	782	550	375	268

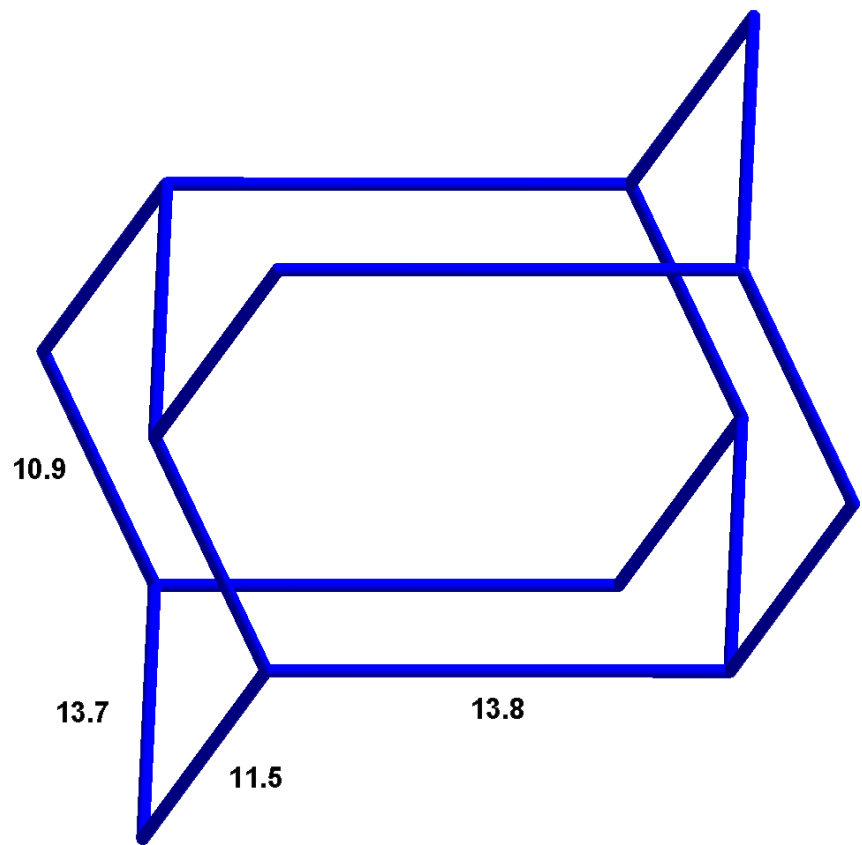


Fig. S1 The adamantanoid cage with wide edges in 3.

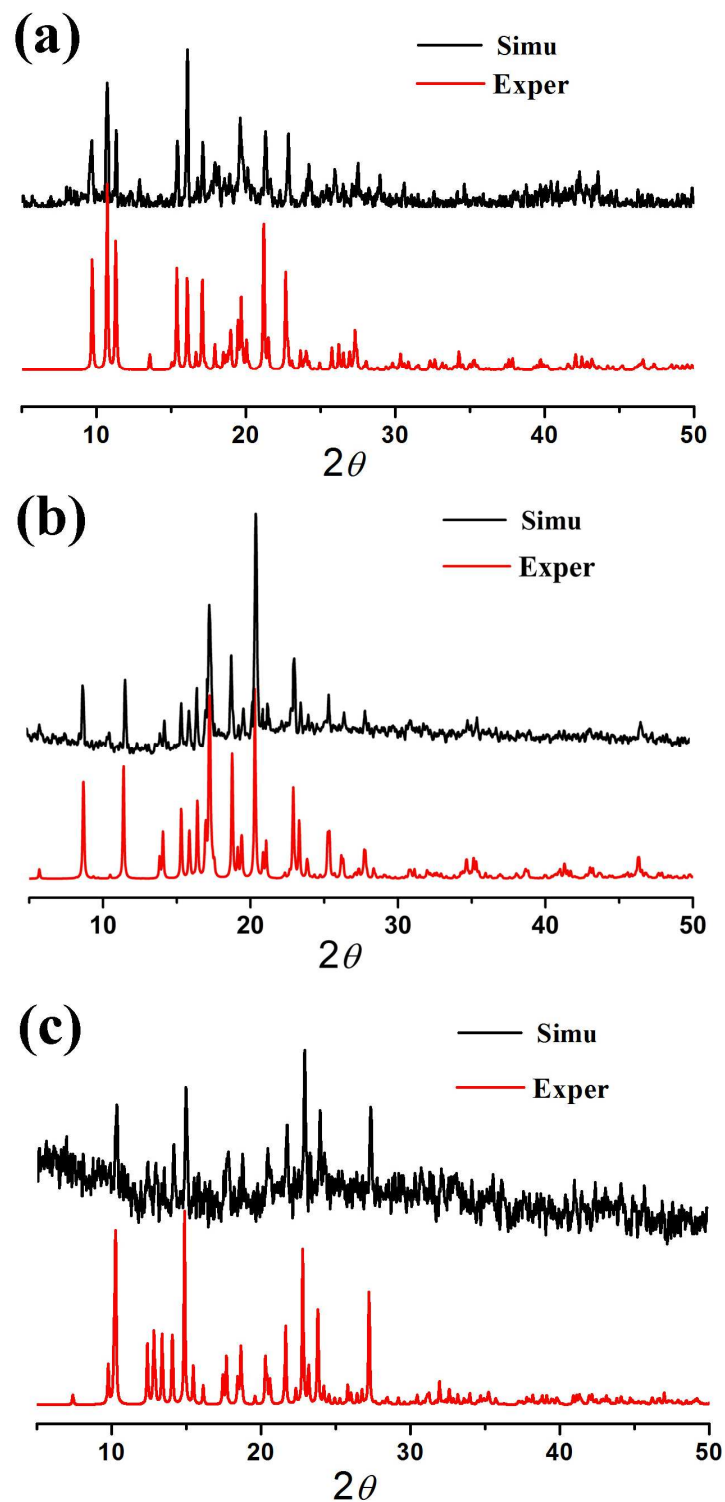


Fig. S2 The simulated and experimental XRD patterns of Co-MOFs (a) 1; (b) 2; (c) 3.

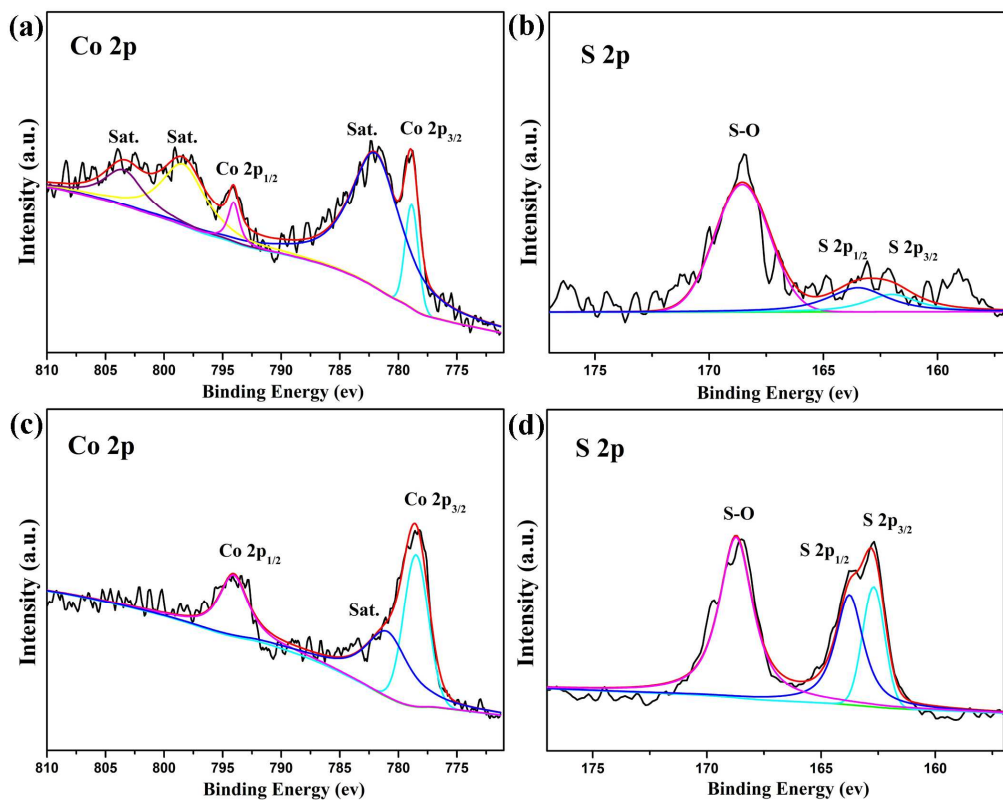


Fig. S3 The Co 2p spectra and S 2p spectra of (a, b) (*o*)-CoS₂@CNT; (c, d) (*m*)-CoS₂@CNT.

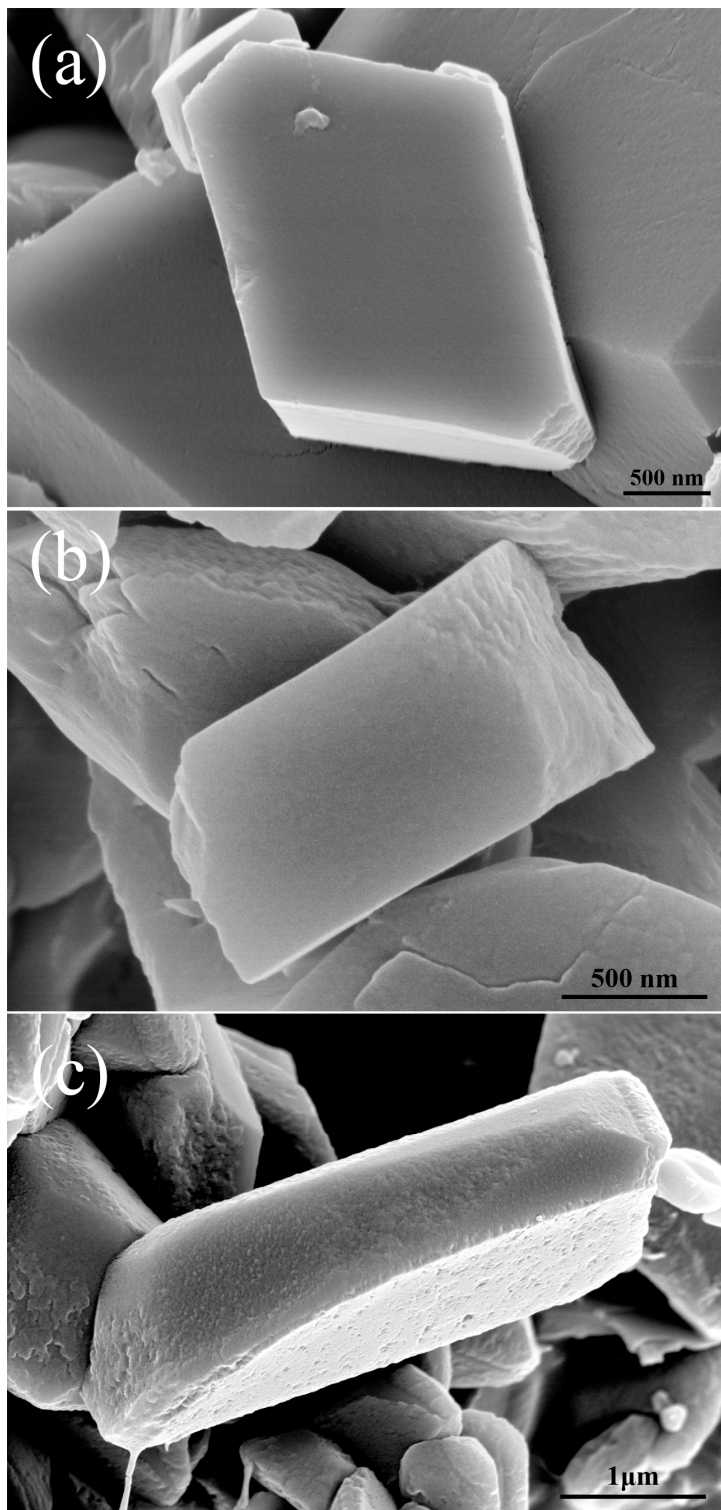


Fig. S4 The FESEM images of Co-MOFs (a) 1; (b) 2; (c) 3.

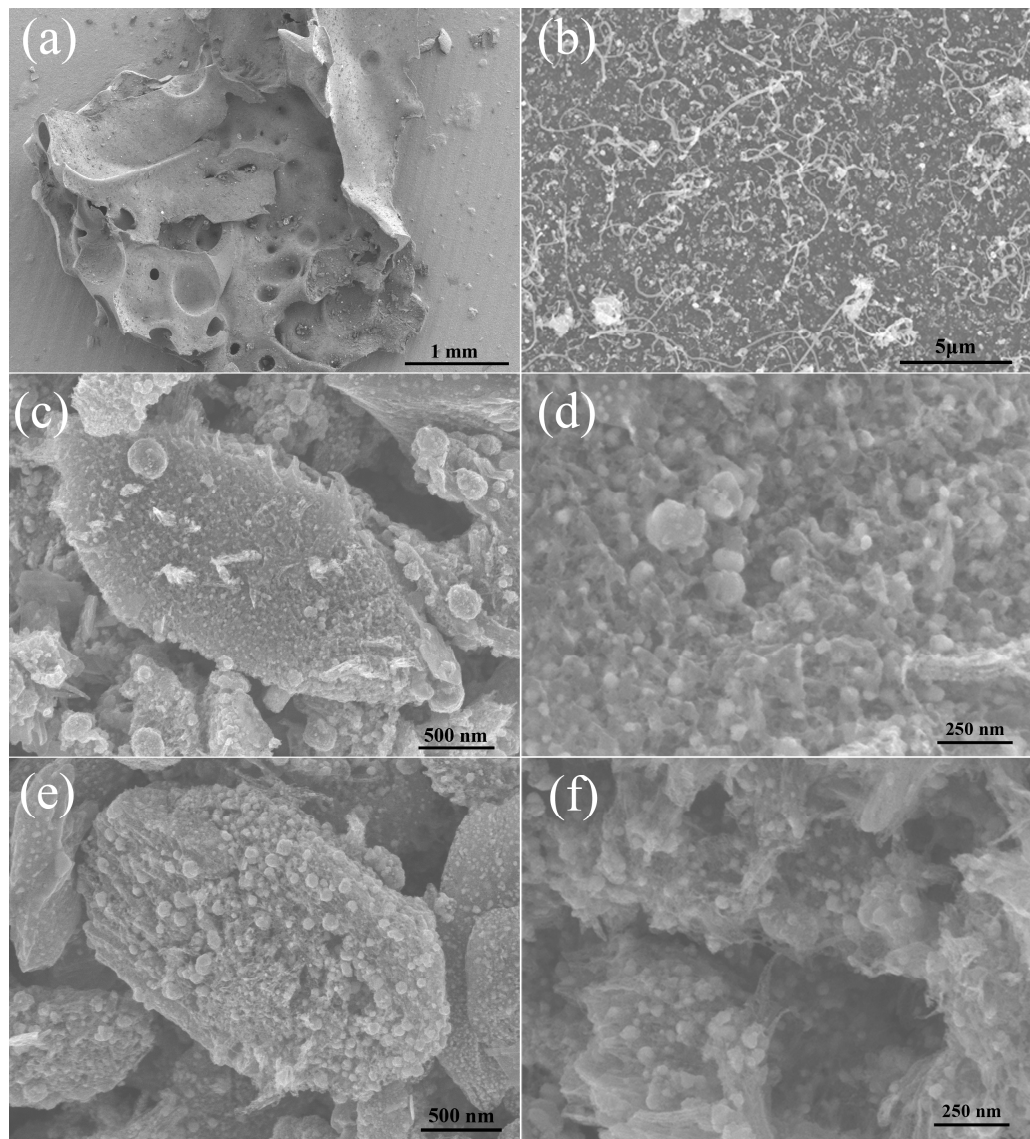


Fig. S5 FESEM images of (a, b) (*o*)-Co@CNT; (c, d) (*m*)-Co@CNT; (e, f) (*p*)-Co@CNT.

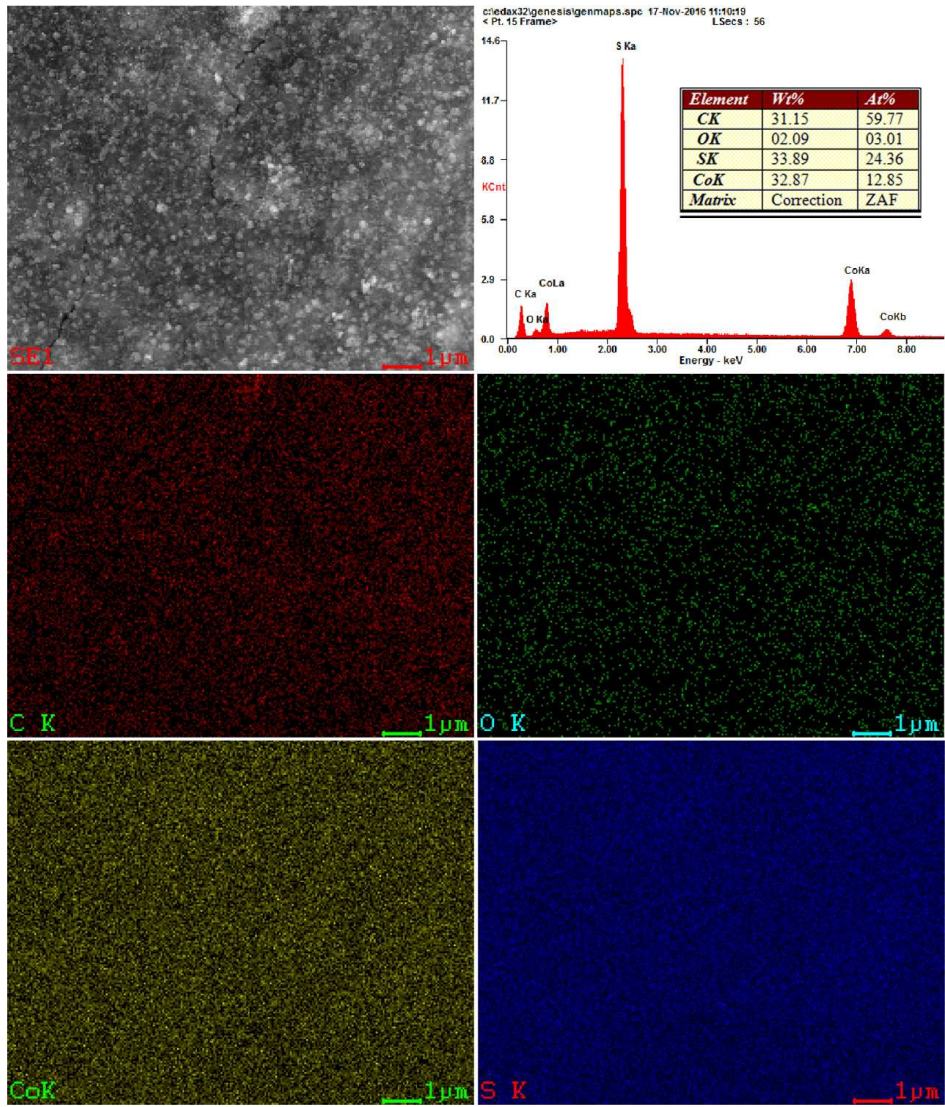


Fig. S6 EDX results of (o)-CoS₂@CNT.

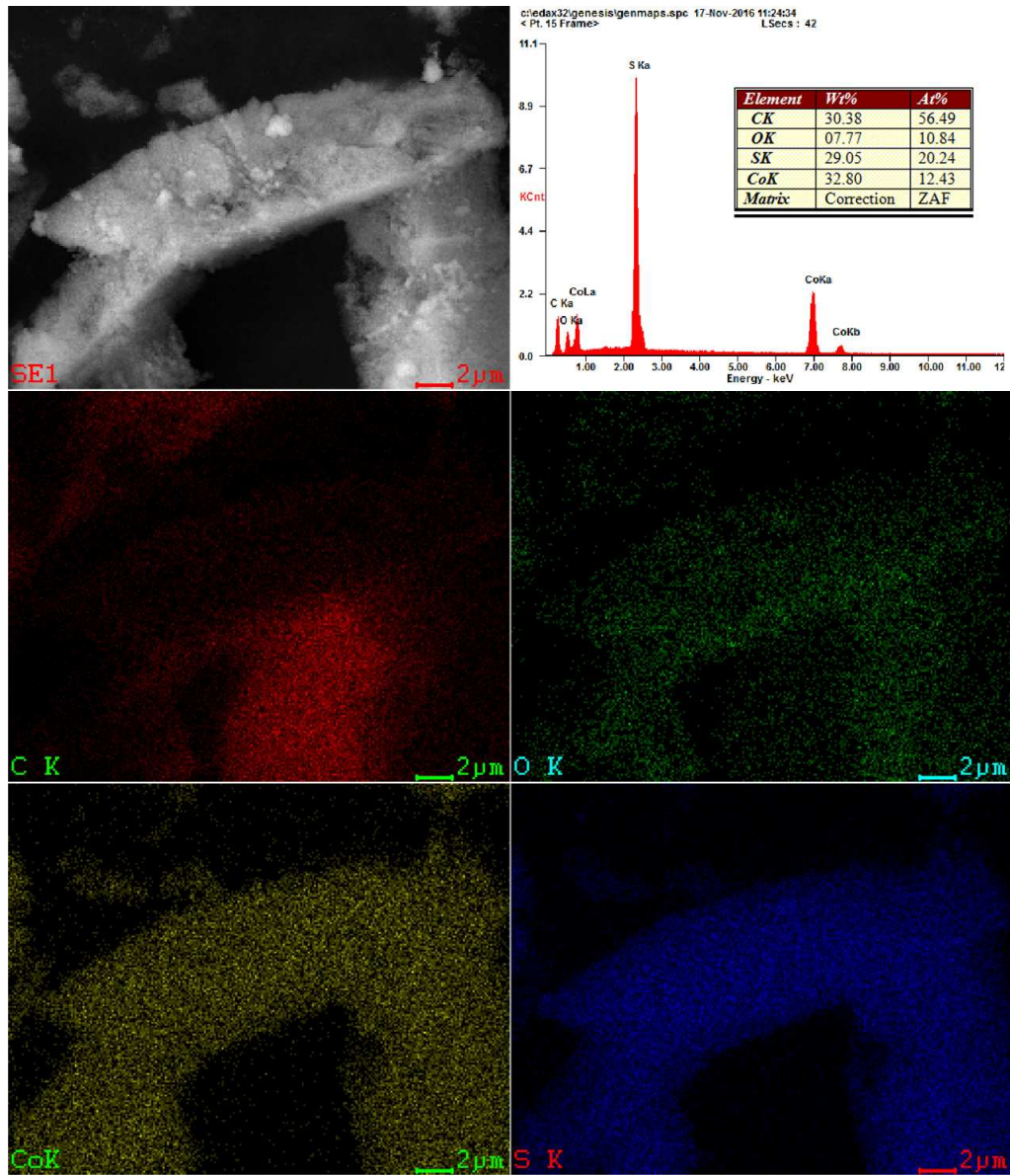


Fig. S7 EDX results of (m)-CoS₂@CNT.

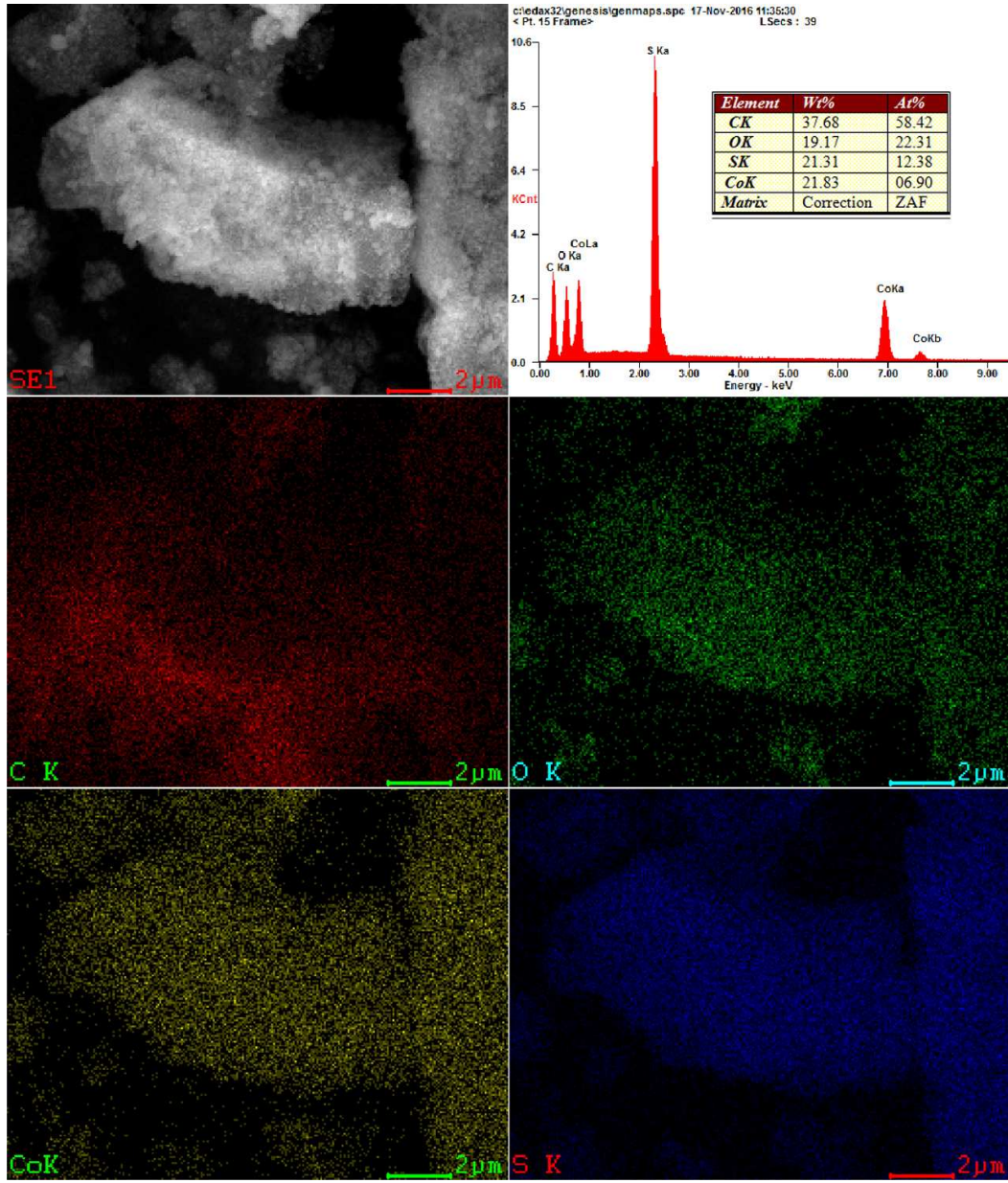


Fig. S8 EDX results of (p)-CoS₂@CNT.

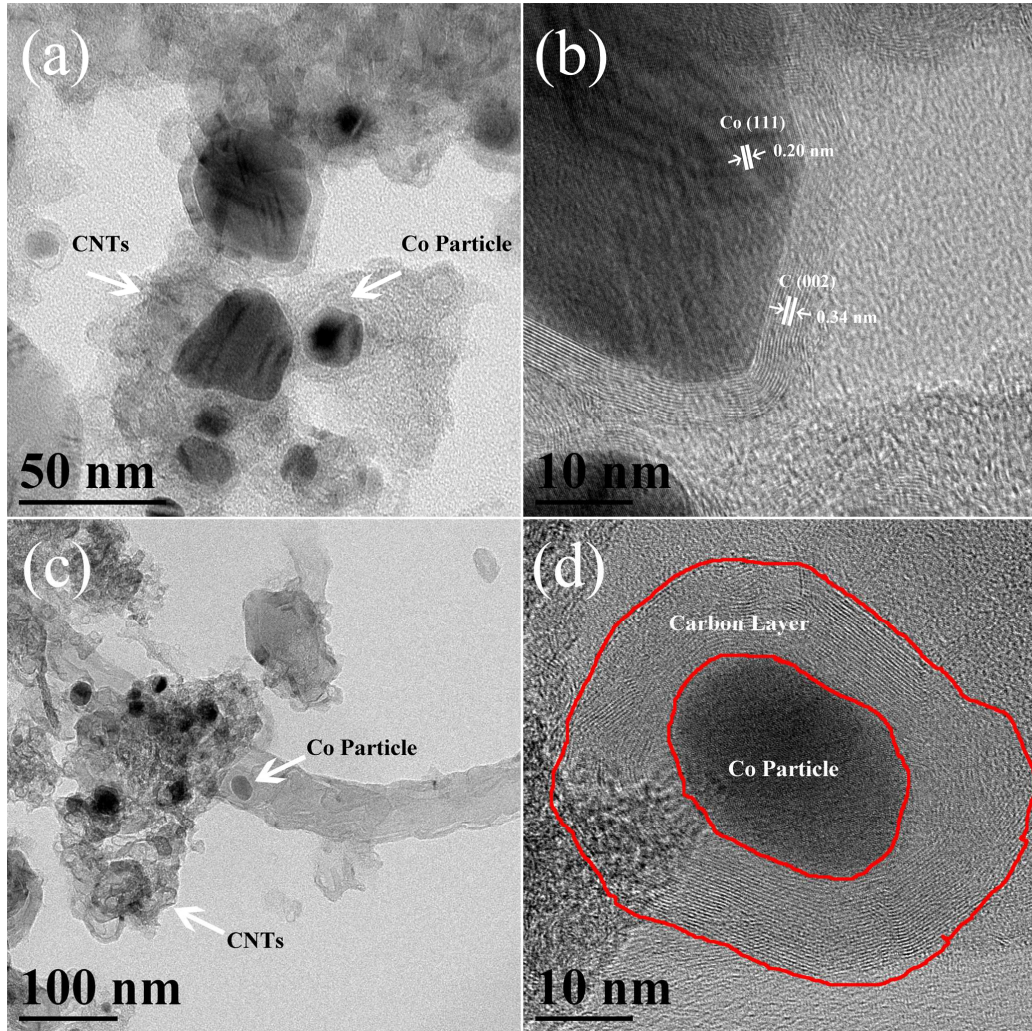


Fig. S9 TEM and HRTEM images of (a, b) (m)-Co@CNT; (c, d) (p)-Co@CNT.

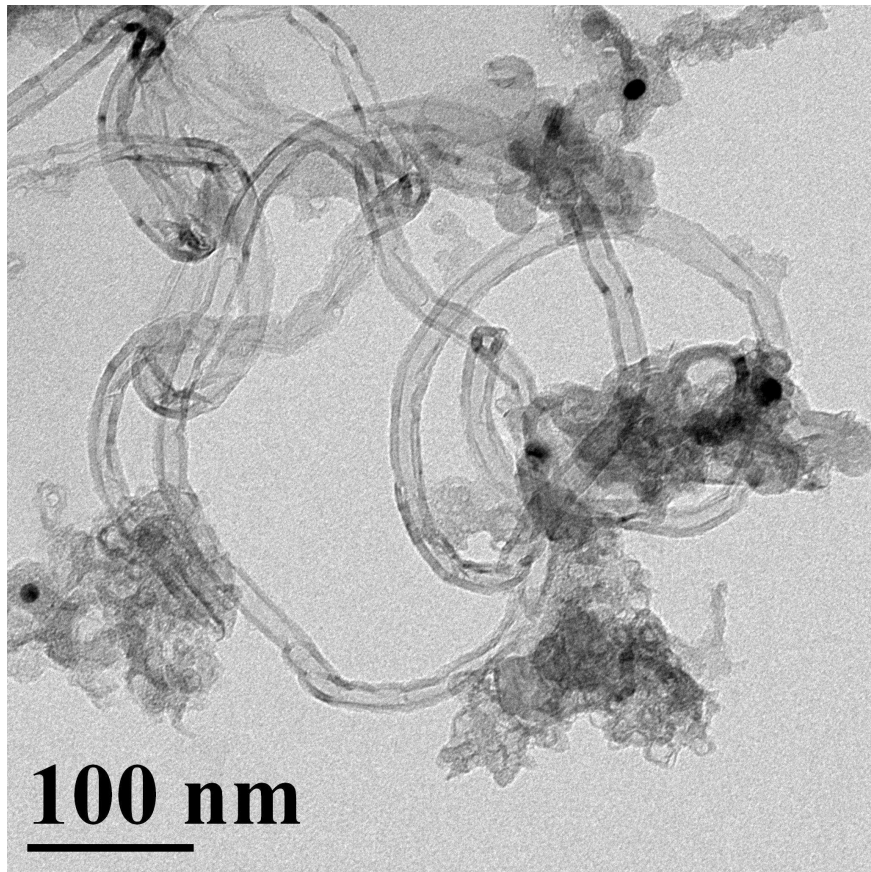


Fig. S10 TEM images of long high-quality CNTs in (p)-Co@CNT.

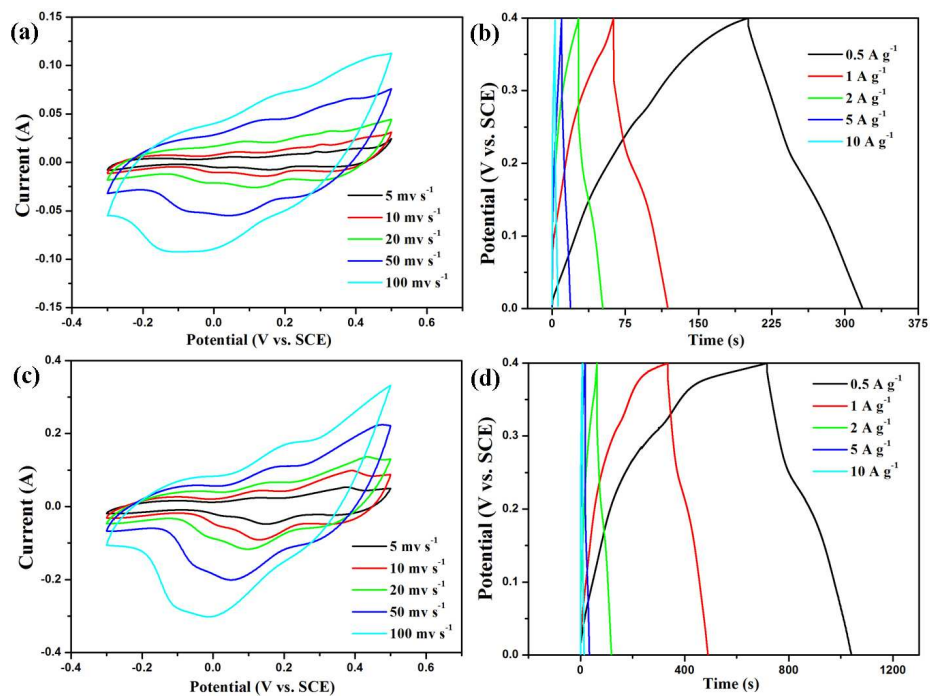


Fig. S11 CV and GCD curves of **(a, b)** (o)-CoS₂@CNT; **(c, d)** (m)-CoS₂@CNT.

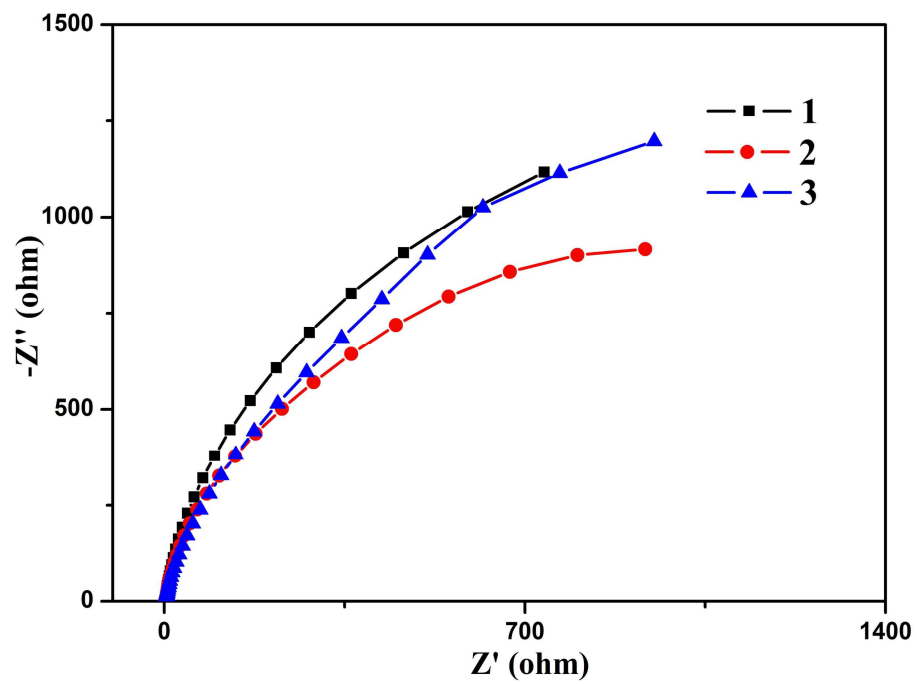


Fig. S12 The Nyquist plots of Co-MOFs.

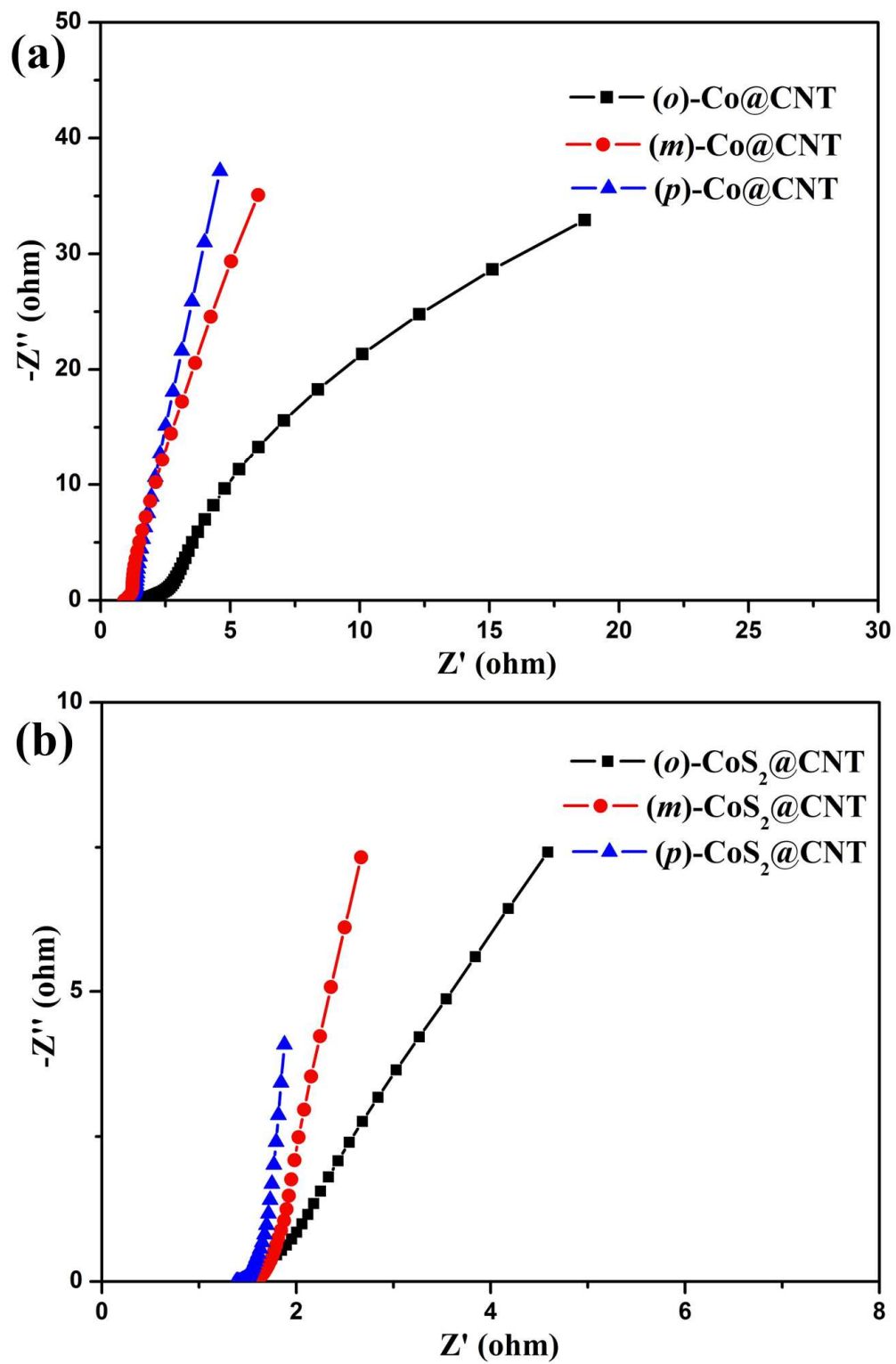


Fig. S13 The Nyquist plots of (a) Co@CNTs; (b) CoS₂@CNTs.